Title
Scanning Josephson Tunneling Microscopy of Single Crystal Bi2Sr2CaCu2O8+delta with a Conventional Superconducting Tip

Author
Kimura, H.

Publication Date
2008-07-18

Peer reviewed

(Title)

Scanning Josephson Tunneling Microscopy of Single Crystal $Bi_2Sr_2CaCu_2O_{8+\delta}$ with a Conventional Superconducting Tip

Hikari Kimura,1,2 R. P. Barber, Jr.,3 S. Ono,4 Yoichi Ando,5 and R. C. Dynes1,2,*

1 *Materials Sciences Division, Lawrence Berkeley National Lab., Berkeley, California 94720, USA*

2 *Department of Physics, University of California, Berkeley, California 94720, USA*

3*Department of Physics, Santa Clara University, Santa Clara, California 95053, USA*

4*Central Research Institute of Electric Power Industry, Komae, Tokyo 201-8511, Japan*

5*The Institute of Scientific and Industrial Research, Osaka University, Ibaraki, Osaka 567-0047, Japan*

(Abstract)

We have performed both Josephson and quasiparticle tunneling in vacuum tunnel junctions formed between a conventional superconducting scanning tunneling microscope tip and overdoped $Bi_2Sr_2CaCu_2O_{8+\delta}$ single crystals. A Josephson current is observed with a peak centered at a small finite voltage due to the thermal-fluctuation-dominated superconducting phase dynamics. Josephson measurements at different surface locations yield local values for the Josephson IcRn product. Corresponding energy gap measurements were also performed and a surprising inverse correlation was observed between the local IcRn product and the local energy gap.

\end{abstract}

(Body)

Remarkable scanning tunneling microscopy (STM) studies on the high-T_C superconducting cuprate (HTSC), $Bi_2Sr_2CaCu_2O_{8+\delta}$ (BSCCO) reveal spectral and energy gap inhomogeneities (1, 2), periodic electronic structure in the superconducting (SC) state (3) and structure inside vortex cores (4) as well as in the "pseudogap" state at temperatures above Tc (5). In these experiments the energy gap Δ is taken to be half the energy separation between the quasiparticle (QP) coherence peaks as observed in dI/dV spectra. The appearance of Δ has also been observed at a temperature T* above Tc with constant ratio $2\Delta /k_BT^*$ (6). The identification of Δ becomes ambiguous, however, in heavily underdoped BSCCO where the observed dI/dV no longer has well defined sharp coherence peaks (7, 8). Two important issues raised by these complex results are (i) whether the SC order parameter of BSCCO has spatial variation, and (ii) how the SC ground state correlates with the QP excited states (Δ). These uncertainties motivate a direct probe of the SC pair wave function. Normal-metal STM studies reveal only the QP excitation spectrum. However, an STM with a SC tip is a local Josephson probe and can, in principle, access the SC pair wave function directly on a length scale smaller than or comparable to the SC coherence length, ξ.

Between conventional superconductors the Josephson IcRn product is a directly measurable quantity uniquely determined by the specific materials in the Josephson junction where, Ic is the critical current and Rn the junction normal-state resistance. This parameter is directly linked to both the SC order parameter amplitude and the energy gaps Δ_{BCS} of the superconductors through the BCS relationship. Josephson studies using a SC-STM on such materials have shown good agreement between the measured IcRn and BCS theory (9, 10). For HTSCs, on the other hand, there is no established theory to relate IcRn with Δ derived from the QP excitation spectrum. IcRn measurements on BSCCO using a SC-STM should, however, both prove the existence and yield the amplitude of the BSCCO pair wave function that couples to the conventional SC tip. Because of the spatial resolution of an STM, this measurement could reveal useful new information regarding inhomogeneity in the superconductivity of BSCCO.

The observation of strong c-axis Josephson coupling in planar Pb -$YBa_2Cu_3O_{7-\delta}$ (YBCO) single crystal Josephson junctions can be explained by an s-wave component in the order parameter of YBCO induced by an orthorhombic distortion (11). Although the crystallographic symmetry of BSCCO makes s- and d-wave mixing less likely, Josephson coupling between conventional superconductors and BSCCO in planar junctions has been observed (12, 13). IcRn values for these junctions (Nb - or Pb -BSCCO) ranged from 1μV to 10μV, indicating that the s-component is about three orders of magnitude smaller than the d-component. Because IcRn was measured in macroscopic junctions, any strong local inhomogeneities were obscured and meaningful comparisons with an inhomogeneous Δ could not be made. It is, therefore, very important to locally probe the order parameter in this strongly inhomogeneous material using Josephson tunneling.

In this Letter we report on direct measurements of the SC ground state of overdoped BSCCO using a SC-STM. Local measurements of both IcRn and Δ were performed. IcRn as a function of Δ tends to decrease as Δ increases. This result is unexpected from BCS theory and consistent with the phase fluctuation model for HTSCs proposed by Emery and Kivelson (14).

The novel feature of our SC-STM is a SC tip (Pb with a Ag capping layer) in close proximity to a SC sample to form a superconductor-insulator-superconductor (S/I/S) tunnel junction (15). The operation of this SC-STM has been demonstrated with the observation of Josephson tunneling between the tip and both SC Pb films (9) and SC $NbSe_2$ (10). The signature Josephson response of the SC-STM differs from that of typical low R_N planar S/I/S devices. Because of the experimental base temperature (T=2.1K) and large R_N associated with an STM, the Josephson binding energy, Ej, which couples the separate SC ground states is smaller than k_BT. For example with an STM resistance of 50kΩ, Ej/k_B is roughly 1K. Also for ultrasmall tunnel junctions, the Coulomb charging energy, Ec can be large. We estimate the capacitance, C, of the STM junction formed between the conical tip apex and the sample surface to be about 1fF. $Ec=e^2/2C$ is therefore of order 1K: comparable with Ej, but smaller than k_BT. Furthermore the time-scale of an electron tunneling in the STM junction is much shorter than $\hbar/Ec$, so that the electron is swept away long before the charging effects become relevant. Because k_BT is the dominant energy, the phase difference of the two superconductors, φ, is not locked in a minimum of the sinusoidal Ej vs. φ washboard potential, but is thermally excited and diffusive. Near zero bias voltage the observed Josephson current is therefore dependent on the bias due to the dissipative phase motion. The experimental data for a Pb film has been explained by a phase diffusion model first proposed by Ivanchenko-Zil'berman (16) and later by others (17, 18). The current–voltage (I-V) characteristics are described by

$$I(V) = Ic^2 Z_{env}/2V/(V^2+Vp^2)), \qquad (1)$$

where the peak in the Josephson current appears at a voltage $Vp=(2e/\hbar)Z_{env}k_BTn$. In this model we can consider the thermal fluctuations as Johnson noise generated by a resistor Z_{env} at temperature Tn; both parameters depend only on the experimental set-up. The observed I-V characteristics for Pb/I/Pb STM Josephson junctions near zero bias with various Rn are fitted to Eq.1 with two parameters, Vp and Ic. This analysis yields a plot of $Ic/((k_BTn)/e)^{1/2}$ vs. Gn=1/Rn, expected to be linear with zero intercept (no Ic at infinite Rn) and a slope equal to $IcRn/((k_BTn)/e)^{1/2}$. Using IcRn(Pb/I/Pb)=1.671 mV (19) known from the Ambegaokar-Baratoff formula (20) and substituting it into the slope of the linear data fit, we can determine Tn and Zenv for our STM Josephson junctions. Current values of these parameters for our apparatus are 15.9 ± 0.1K and $279\pm9\Omega$, respectively.

Using our well-characterized SC-STM, we have studied overdoped BSCCO single crystals with Tc values of 76K, 79K and 81K. Samples are cleaved in ultrahigh vacuum and cooled to T=2.1K. Because of the thick Pb layer used in our SC tip fabrication, we rarely observe atomic resolution images. However we can easily locate step edges and isolate flat surfaces where all the present data were measured. We first observe the dI/dV spectrum at a particular surface point on sample 1 (Tc = 79K) to measure the BSCCO energy gap Δ (black line in the Inset of Fig. 1). We use standard Lock-in techniques with 1KHz modulation on the bias voltage and an Rn ~ 500MΩ. Although a simplification of a more complex structure, we use the same definition for Δ as in previous works in order to make comparisons. In the main frame we plot the I-V characteristics at lower bias and lower Rn. A low leakage current below the Pb gap confirms high quality vacuum tunnel junctions. Further decreasing Rn increases the QP tunneling probability and finally the thermally fluctuated Josephson currents are observed when Ej is comparable to k_BTn. The QP background inside the Pb gap is much larger than that of Pb/I/Pb STM Josephson junctions because of the gaplessness of the local density of states (LDOS) of BSCCO.

Fig. 2(a) displays a close-up view of the I-V characteristics near zero bias, clearly showing that the SC Pb tip was Josephson coupled to the BSCCO. The averaged QP background is represented by the red line in Fig. 2(b). Fig 2(c) shows the contributions from the thermally fluctuated Josephson current after subtracting the QP background of Fig 2(b) from the I-V curves of Fig 2(a). The data in Fig 2(c) are shown as lines and the best fits to Eq. (1) are represented by the symbols. These good fits convince us that we have observed the pair current between a conventional (s-wave) SC Pb tip and overdoped BSCCO, suggesting that the BSCCO does not have a pure d-wave order parameter. In addition, the dI/dV represented by the red line in the Inset of Fig. 1 was observed after low Rn measurements in Fig. 2. The LDOS was changed significantly during the measurements; and the QP coherence peaks have disappeared, perhaps due to the high current density of the measurements at the highest conductances studied. This dI/dV resembles those previously observed in heavily underdoped BSCCO (6-8), and in the "pseudogap" state at temperatures above Tc (21). It is also similar to the dI/dV spectra observed by others on surfaces which were altered by scanning with large tunnel currents (22). It is important to note that LDOS changes were observed only when measurements were made with Rn below 30kΩ. In order to avoid this effect, most of the data presented here were obtained with Rn ranging from 30kΩ to 100kΩ.

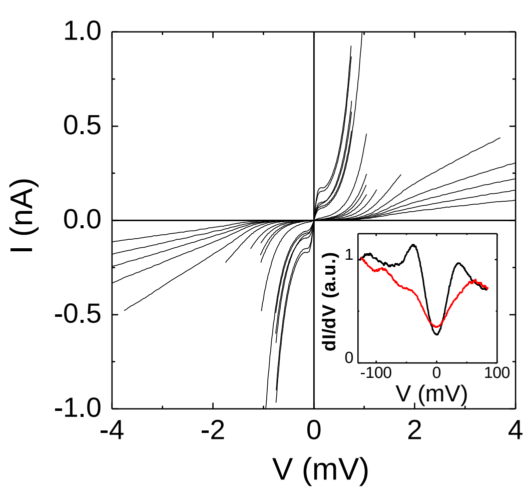

Fig.1 I-V characteristics of Pb/I/overdoped BSCCO (Tc=79K) STM Josephson junctions at T=2.1K. The Pb gap is clearly seen around V=1.4mV. Inset: dI/dV spectrum (black line) measured before low Rn measurements, showing sharp coherence peaks with Δ=37meV. dI/dV measured after low Rn measurements (red line) indicates an LDOS change due to high current density.

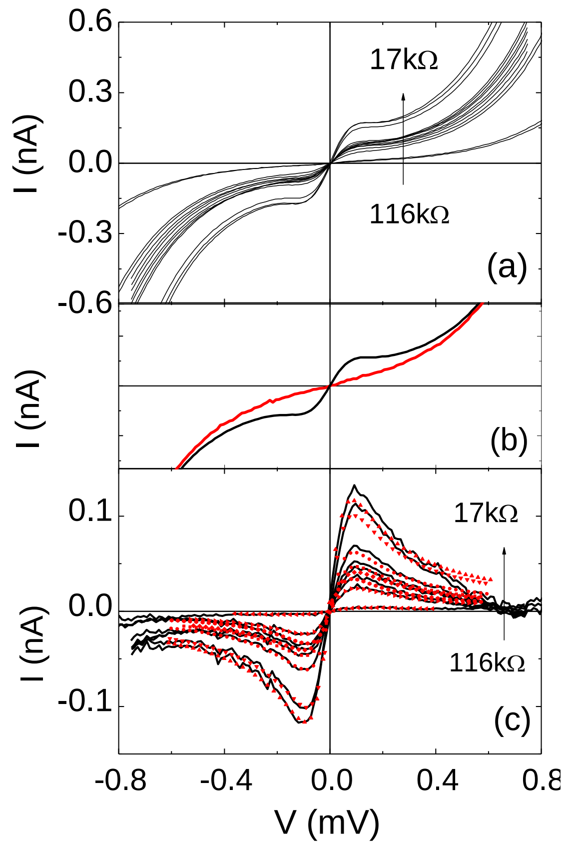

Fig. 2 (a) Low bias I-V characteristics of Fig 1 for various junction resistances at T=2.1K. (b) Averaged I-V characteristic near zero bias for quasiparticle background (red line). One of the observed I-V curves is shown by the black line. (c) Thermally fluctuated Josephson currents peaked at Vp as derived by subtracting quasiparticle background (Fig 2b) from the I-V curves (Fig 2a). The data are represented by the lines and the symbols represent two-parameter fits to the phase diffusion model.

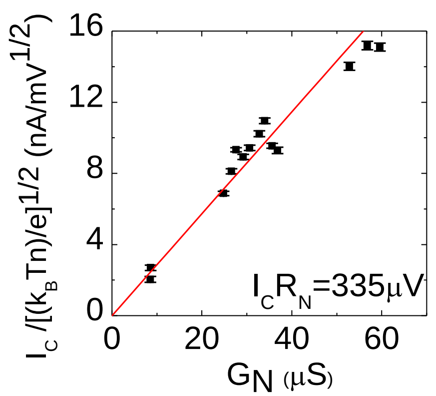

Fig. 3 Plot of $Ic/\{(k_BTn)/e\}^{1/2}$ vs. Gn. The slope is equal to $IcRn/\{(k_BTn)/e\}^{1/2}$. Using the fitted slope and substituting the previously determined Tn, the Josephson product at this surface point is found to be IcRn=335μV

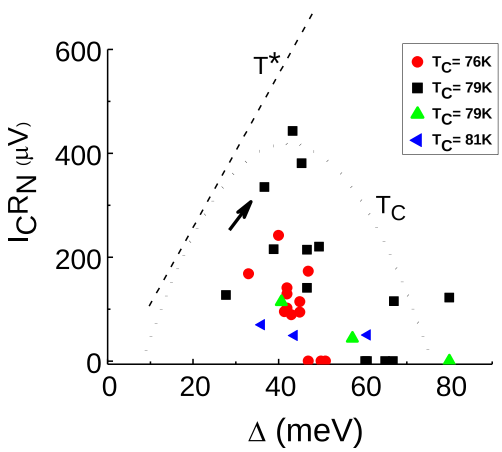

Fig. 4 IcRn as a function of Δ. Each data point represents a separate measurement from a different location over 4 different samples. The IcRn value derived from Fig. 3 is one of the black square symbols denoted with an arrow. All other points are derived similarly. IcRn appears to be a maximum for Δ between 40 and 45 meV, while it decreases for larger and smaller Δ. Sketches of Tc and T* from the Emery-Kivelson model are shown by dotted and dashed lines, respectively. The vertical scale for the model curves is arbitrary.

A fit to each I-V curve in Fig. 2 (c) generates a single data point in the plot shown in Fig. 3. As Gn is increased (Rn is reduced) the observed Ic increases (Ej increases). Using the previously determined Tn and Zenv and the slope of the linear fit shown in Fig 3, we find IcRn at this surface point to be 335μV. It is important to note that low Rn measurements (Rn below ~ 300kΩ) on BSCCO increase the low frequency noise on the tunnel current. This noise appears to be induced locally on the BSCCO and not from the environment or electronics. We assure that we have not affected the tip during the measurements by verifying that the Pb gap is always reproduced and exponential decay of the tunnel current vs. the tip-sample distance is also observed after low Rn measurements.

Fig. 4 summarizes Josephson IcRn product vs. Δ measurements for four overdoped samples with each data point taken at locations roughly 10Å apart. Although there is scatter in the observed IcRn values for a given Δ, this figure clearly indicates the nanometer scale inhomogeneities in both IcRn and Δ. The reason for the scatter from experiment to experiment is under investigation. The notable result in Fig. 4 is that IcRn tends to be a maximum when Δ is between 40 and 45meV, and the trend is for it to decrease or become zero as Δ increases or decreases from this maximal point.

We interpret these results within the framework of the phase diagram for HTSCs proposed by Emery and Kivelson (E-K model) (14). In this picture Tc vs. hole doping, δ, in the SC region has a dome shape with the maximum Tc at δ~0.16. Changing δ from this value results in a Tc decrease. Another parameter, T* is described as the temperature below which a gap in the QP spectrum is formed, but without long-range phase coherence. T* continues to rise as δ decreases and Tc decreases.

In order to overlay this phase diagram on our Fig. 4, we make two assumptions. First, we note that T* decreases monotonically as δ increases. Using previous results that Δ/T* is observed to remain constant for optimally-doped and overdoped BSCCO (6), we can transform the model's δ-axis into the Δ-axis in our Fig. 4. Now T* monotonically increases and the dome-shaped region is simply flipped horizontally as shown when plotted vs. Δ. Second, we assume that parameters for each sample location are correlated with the locally measured Δ and therefore the corresponding doping which produces samples with the same average behavior. For example, Fig. 4 indicates that IcRn is maximized at a gap value of 40~45meV, the average Δ typically observed in optimally-doped BSCCO (corresponding to the highest Tc samples). IcRn decreases as Δ becomes larger or smaller than this value, and therefore follows a trend similar to that of the Tc curve in the model. It is important to reiterate that for any given sample, we observed inhomogeneities both in Δ and IcRn as a function of location.

From our results we correlate the observed IcRn with the amplitude of the SC order parameter |Ψ| as well as with the Tc of BSCCO via the E-K model phase diagram. These three quantities

(IcRn, |Ψ| and Tc) decrease (smaller superfluid density) as Δ increases and anticorrelate with T*. This inverse relation between IcRn and Δ in BSCCO is an unconventional result because in the BCS model Δ_{BCS}, IcRn, |Ψ| and Tc are all correlated. We observe a more conventional behavior in the overdoped (amplitude dominated) side of the phase diagram. Here both Tc and Δ decrease as δ is increased above 0.16. In this regime (the averaged Δ ≤ 40 meV), T* and IcRn closely relate to Δ so that IcRn, |Ψ|, Tc, Δ and T* all behave similarly.

Another possible framework for discussing our results is the two-gap scenario (23). In the underdoped regime, this picture conjectures that the large gap observed in the pseudogap phase is distinct from the genuine superconducting gap that tracks Tc. Although consistent with our IcRn measurements, we do not observe the second gap directly. Since the results in Fig. 4 represent measurements of *both* IcRn and Δ averaged over momentum space, we are unable to do the same local comparison to address this alternate model.

In summary we have observed the thermally fluctuated Josephson current for c-axis tunneling between a SC Pb tip and overdoped BSCCO single crystals. To our knowledge this is the first local Josephson measurement along the c-axis between s- and d-wave superconductors. Probing both IcRn and Δ over the surface indicates an anticorrelation between the Josephson coupling and Δ. This result is consistent with the E-K phase fluctuation model for a low superfluid density superconductor.

The authors acknowledge assistance and helpful conversations with Mike Crommie, John Clarke and Ofer Naaman. We thank Paul Reichardt and Darin Kinion for the cryogenic microwave filter design and the Berkley Physics Machine shop for expert technical assistance. This work was supported by the Director, Office of Science, Office of Basic Energy Sciences, Materials Sciences and Engineering Division, of the U.S. Department of Energy under Contract No. DE-AC02-05CH11231 and DOE Grant No. DE-FG02-05ER46194. Ono was supported by KAKENHI 20740213 and Ando by KAKENHI 19674002.

[1] S. H. Pan *et al.*, Nature (London) **413**, 282 (2001).
[2] K. M. Lang *et al.*, Nature (London) **415**, 412 (2002).
[3] J. E. Hoffman *et al.*, Science **297**, 1148 (2002).
[4] J. E. Hoffman *et al.*, Science **295**, 466 (2002).
[5] M. Vershinin *et al.*, Science **303**, 1995 (2004).
[6] K. K. Gomes *et al.*, Nature (London) **447**, 569 (2007).

[7] K. McElroy *et al.*, Phys. Rev. Lett. **94**, 197005 (2005).

[8] J. W. Alldredge *et al.*, Nat. Phys. **4**, 319 (2008).
[9] O. Naaman, W. Teizer, and R. C. Dynes, Phys. Rev. Lett. **87**, 097004 (2001).
[10] O. Naaman, R. C. Dynes, and E. Bucher, Int. J. Mod. Phys. B **17**, 3569 (2003).
[11] A. G. Sun *et al.*, Phys. Rev. Lett. **72**, 2267 (1994).

[12] M. M¨oßle and R. Kleiner, Phys. Rev. B **59**, 4486 (1999).
[13] I. Kawayama *et al.*, Physica C **325**, 49 (1999).
[14] V. J. Emery and S. A. Kivelson, Nature (London) **374**, 434 (1995).
[15] O. Naaman, W. Teizer, and R. C. Dynes, Rev. Sci. Instrum. **72**, 1688 (2001).
[16] Y. M. Ivanchenko and L. A. Zil'berman, Zh. Eksp. Teor. Fiz. **55**, 2395 (1968).
[17] Y. Harada, H. Takayanagi, and A. A. Odintsov, Phys. Rev. B **54**, 6608 (1996).
[18] G.-L. Ingold, H. Grabert, and U. Eberhardt, Phys. Rev. B **50**, 395 (1994).
[19] We use Δ_{Pb}=1.35mV and include a factor of 0.788 due to strong phonon coupling in Pb.
[20] V. Ambegaokar and A. Baratoff, Phys. Rev. Lett. **10**, 486 (1963).
[21] C. Renner *et al.*, Phys. Rev. Lett. **80**, 149 (1998).
[22] C. Howald, P. Fournier, and A. Kapitulnik, Phys. Rev. B **64**, 100504 (R) (2001).
[23] W. S. Lee *et al.*, Nature (London) **450**, 81 (2007).